Dynamics of Atmospheres and Oceans 52 (2011) 322–340

Contents lists available at ScienceDirect

Dynamics of Atmospheres and Oceans

journal homepage: www.elsevier.com/locate/dynatmoce

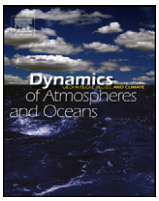

On the modeling of the 2010 Gulf of Mexico Oil Spill

A.J. Mariano[a,*], V.H. Kourafalou[a], A. Srinivasan[a,d], H. Kang[a], G.R. Halliwell[b], E.H. Ryan[a], M. Roffer[c]

[a] University of Miami Rosenstiel School of Marine and Atmospheric Science, United States
[b] NOAA Atlantic Oceanographic and Meteorological Laboratory, United States
[c] Roffer's Ocean Fishing Forecasting Service, Inc. (ROFFS™) & Florida Institute of Oceanography, United States
[d] Center for Computational Science, University of Miami, Miami, Florida.

ARTICLE INFO

Available online 19 August 2011

Keywords:
Numerical model
Lagrangian trajectory prediction
Oil spill

ABSTRACT

Two oil particle trajectory forecasting systems were developed and applied to the 2010 Deepwater Horizon Oil Spill in the Gulf of Mexico. Both systems use ocean current fields from high-resolution numerical ocean circulation model simulations, Lagrangian stochastic models to represent unresolved sub-grid scale variability to advect oil particles, and Monte Carlo-based schemes for representing uncertain biochemical and physical processes. The first system assumes two-dimensional particle motion at the ocean surface, the oil is in one state, and the particle removal is modeled as a Monte Carlo process parameterized by a one number removal rate. Oil particles are seeded using both initial conditions based on observations and particles released at the location of the Maconda well. The initial conditions (ICs) of oil particle location for the two-dimensional surface oil trajectory forecasts are based on a fusing of all available information including satellite-based analyses. The resulting oil map is digitized into a shape file within which a polygon filling software generates longitude and latitude with variable particle density depending on the amount of oil present in the observations for the IC. The more complex system assumes three (light, medium, heavy) states for the oil, each state has a different removal rate in the Monte Carlo process, three-dimensional particle motion, and a particle size-dependent oil mixing model.

* Corresponding author.
E-mail address: amariano@rsmas.miami.edu (A.J. Mariano).

0377-0265/$ – see front matter
doi:10.1016/j.dynatmoce.2011.06.001

Simulations from the two-dimensional forecast system produced results that qualitatively agreed with the uncertain "truth" fields. These simulations validated the use of our Monte Carlo scheme for representing oil removal by evaporation and other weathering processes. Eulerian velocity fields for predicting particle motion from data-assimilative models produced better particle trajectory distributions than a free running model with no data assimilation. Monte Carlo simulations of the three-dimensional oil particle trajectory, whose ensembles were generated by perturbing the size of the oil particles and the fraction in a given size range that are released at depth, the two largest unknowns in this problem. 36 realizations of the model were run with only subsurface oil releases. An average of these results yields that after three months, about 25% of the oil remains in the water column and that most of the oil is below 800 m.

1. Introduction

Following the tragic Deepwater Horizon oil rig explosion on April 20, 2010, oil gushed from the bottom of the Gulf of Mexico at a depth of 1500 m, latitude 28.74°N and longitude 88.32°W, for 87 days before it was capped. The gushing Mississippi Canyon (MC) 252 oil is a complex mixture of hydrocarbons and other trace compounds with a mean density of about 0.85 g/cm^3, lighter than the surrounding seawater that has a density of about 1.03 g/cm^3 (Deepwater Horizon MC 252 Response Unified Area Command, 2010). A buoyant plume is driven by gases that are gushing out of the broken pipes and by the density difference between the oil/gas mixture and the surrounding seawater. The official time-varying flow rate, announced on August 2, 2010, decreased from an initial rate of 62,000 to a final rate of 53,000 barrels of oil per day, for a total release of 4.9 million barrels of oil from the well, though as much as 25,000 barrels per day were collected by surface ships during the latter part of the oil spill (McNutt et al., 2011). Peak flow rates are about 10^4 m^3 a day with an uncertainty in the flow rate estimates of ±10%. The surface slick, first seen on April 22, 2010, quickly spread to a slick with a surface area of about 17,725 km^2 on May 17, 2010 based on the analysis of a multichannel MODIS (MODerate-resolution Imaging Spectroradiometer) satellite image (Labson et al., 2010). On the average, NOAA and the USCG estimated that 2% of the oil was thick, 10% was characterized as dull, and 88% was classified as sheen (Labson et al., 2010). The temporal evolution of the spatial extent of the oil spill, and a measure of the error of that estimate, will be needed for the natural resource damage assessment such as quantifying the oil that is impacting marine habitats.

There are a number of different satellite, in situ, and model-based estimates of the location of the oil. There are considerable differences in the oil location between these estimates (see Fig. 1) and each estimate exhibits significant variation in a temporal sequence of oil location maps. In situ observations are limited by available resources, large search domain, weather, and observing error. High-resolution visible and infra-red images of the upper few millimeters of the ocean surface can be obscured by clouds, while microwave-based measurements with a coarser sampling resolution of 25 km would miss oil filaments, for example, seen in other observations. SAR images work best in limited wind regimes (Brekke and Solberg, 2005) between 3 and 10 m/s, with best results for winds around 5–6 m/s. At low wind speeds, there is a high probability of oil slick look-alikes due to local wind variability, and at higher wind speeds, light oil is mixed and dispersed.

The identification of the location of the oil spill is further complicated by the fact that locations with no oil can be due to either no reliable observations in that region or highly accurate observations of no oil found in the region. Fig. 1a and b is the most complete estimate of oil locations incorporating the most observations. Fig. 1c shows a composite of 2 SAR images for June 11, 2010 from CSTARS that contains very detailed oil locations where data are available, but complete data voids in areas where oil was observed in the other data sets. Fig. 1d is a composite based on satellite images (Section 3)

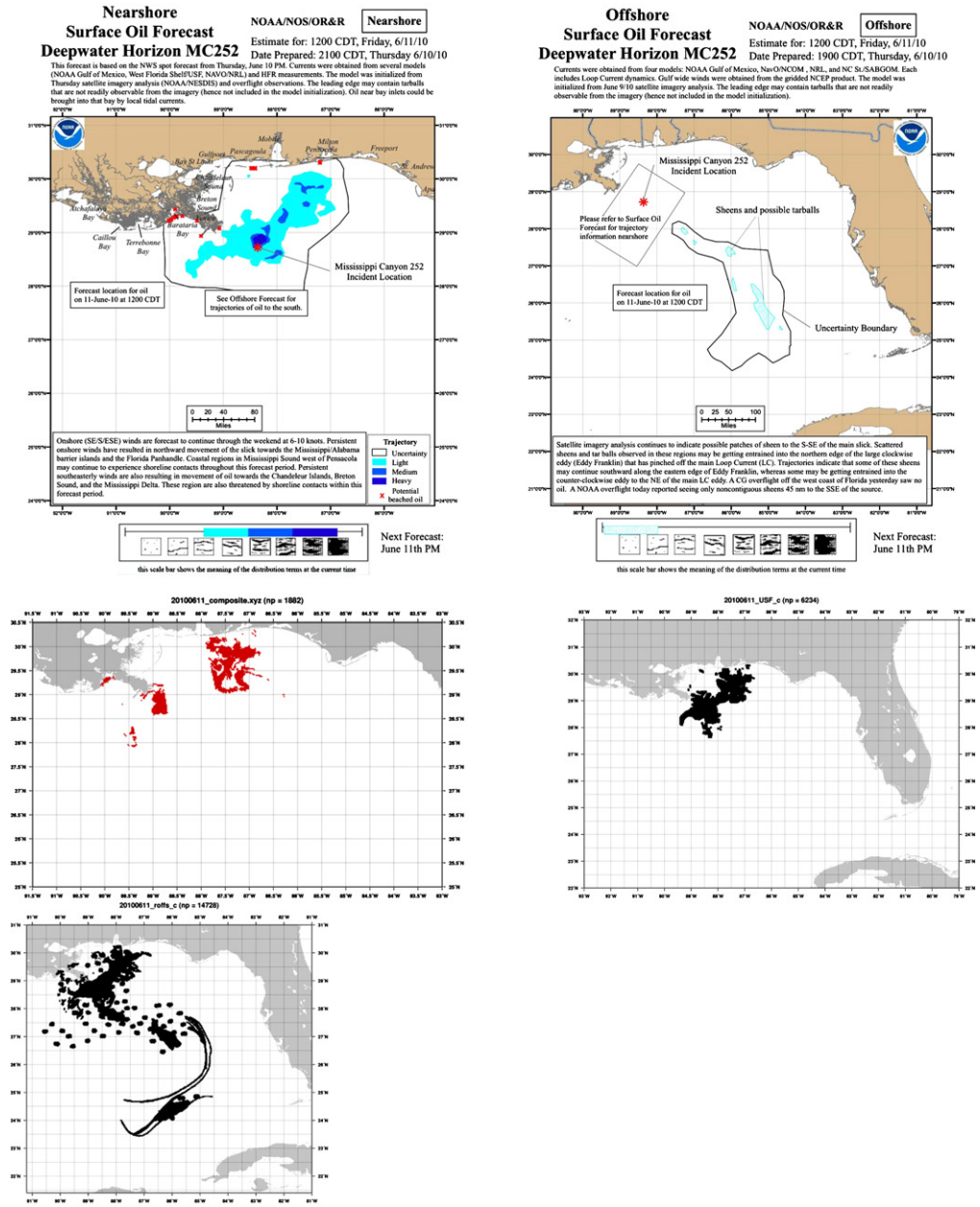

Fig. 1. The top two panels are NOAA's 24 h forecast of oil location for June 11, 2010. The digitized versions of estimates of oil location by U. Miami CSTARS (middle left panel) and U. South Florida (middle right panel), and ROFFS^{TM} (bottom panel). There is considerable variability among the four different analyses for this day and also for the other days (see Figs. 3–5).

from C. Hu (USF) that is most similar with the NOAA trajectory estimates (Fig. 1a). Fig. 1e is an analysis (Section 3) done by Roffer's Ocean Fishing Forecasting Service, Inc. (ROFFS^{TM}) that contains more oil in the far field than the other estimates. Oil location estimates Fig. 1a and e also vary with respect to the characteristics of the oil, *e.g* thick oil versus light sheen. Consequently, estimating oil location from

observations, that are used for initial conditions, data assimilation, and as truth for benchmarking numerical simulations of oil trajectories, is difficult and different approaches should be evaluated.

Oil is not a conservative tracer since it undergoes physical and chemical changes called "weathering" due to wind- and wave-enhanced mixing, evaporation, sedimentation/sinking, dissolution, re-suspension, emulsification, photo-oxidation, and biodegradation (Scholz et al., 1999). Emulsification slows down the removal process and results in heavy, mousse colored waters and tar balls/patties/lumps/mats, and these end products can account for 10–25% of the oil. In particular, tar mats can form on the bottom on the order of 5 cm thick and this typically accounts for 2–5% of the oil. Larger subsurface oil droplets are formed by turbulent enhanced mixing of emulsified fluid and this process can account for 10–20% of the oil (Scholz et al., 1999). The use of dispersants enhances the formation of oil droplets in the water column. The National Incident Command for this spill estimated that 30% of the dispersant-laden leaked oil is dispersed in the water column as oil droplets (Lubchenco et al., 2010). Historical estimates of evaporation range from 20 to 80% of oil evaporating during the first week after the oil surfaces and then evaporation becomes a slower process (Scholz et al., 1999). The National Incident Command for this spill estimated that 25% of the oil evaporated, 17% was recovered by siphoning into ships, and approximately 10% of the oil was also being removed by clean-up crews using methods including suction hoses, skimming boats, and controlled burning. 16% and 8% of the oil was naturally and chemically dispersed in the water column, respectively, and that 26% of the oil was "residual" and is sheen, tar balls, washed ashore, or is buried in sand and sediments (Lubchenco et al., 2010). Photo-oxidation and biodegradation are both slow, steady processes that will remove the residual and dispersed oil with biodegradation being the most important on the longest time-scales of year(s). There may be microbes that are more efficient at biodegradation or that oil concentrated in subsurface plumes may lead to more microbes (Hazen et al., 2010; Camilli et al., 2010) and this time scale may be months.

In reality, a tertiary fluid model (water, salt, oil) would be needed for the most realistic oil spill model since the amount of oil created significant frontal regions where the horizontal density difference between water and oil governed the local fluid dynamics. These regions are evident in aerial images of the spill. In practice, oil weathering models are coupled to numerical circulation models to include these nonconservative processes, *e.g.* STATMAP (Skognes and Johansen, 2004), GNOME (NOAA, 2002), and OILMAP from Applied Science Associates. However, an incomplete understanding of the weathering processing and of turbulent mixing introduces the need for weathering and sub-grid scale parameterizations in all oil spill models. These parameterizations require the estimation of empirical coefficients that depend on both the type and age of oil, and on environmental factors such as wind speed, temperature, wave height, and salinity. Uncertainties in parameterizations used in these models, initial conditions, and environmental data all lead to uncertainties in estimates of oil locations and state. This is especially true in new settings such as a deep spill laced with dispersants or when there are significant errors in the environmental data. Thus it may be advantageous to run less complex models, that parameterize the main error sources and unresolved processes, by perturbing parameters, initial conditions, flow rates, and/or advective velocities to generate ensembles of oil trajectories that can be analyzed. Monte Carlo based averages of oil location may be as accurate as coupled circulation–oil weather models.

Two Lagrangian trajectory simulations models with increasing level of complexity on the parameterization of particle properties and of the processes controlling the particle trajectories, have been developed. The first model assumes only one oil state and that the oil is passively advected and dispersed by the two-dimensional horizontal velocity fields from the hydrodynamic model and by a Lagrangian-based stochastic parameterization of the unresolved velocity fields. A Monte Carlo approach for parameterizing the net effects of oil weathering and removal is introduced and evaluated in the two-dimensional simulations. The second model simulates three-dimensional oil trajectories with particles that can also have three states; light, medium and heavy oil. The three-dimensional model incorporates more processes and uses a Monte Carlo approach for weathering and for perturbing flow rates and the oil state, as well as, the Lagrangian stochastic models to represent uncertainties in the velocities from the hydrodynamical model (Section 2).

It is well-known that due to the nonlinearity of Lagrangian motion in the geophysical fluids, the reliable prediction of particle trajectories is limited to about twice the Lagrangian integral time scale of

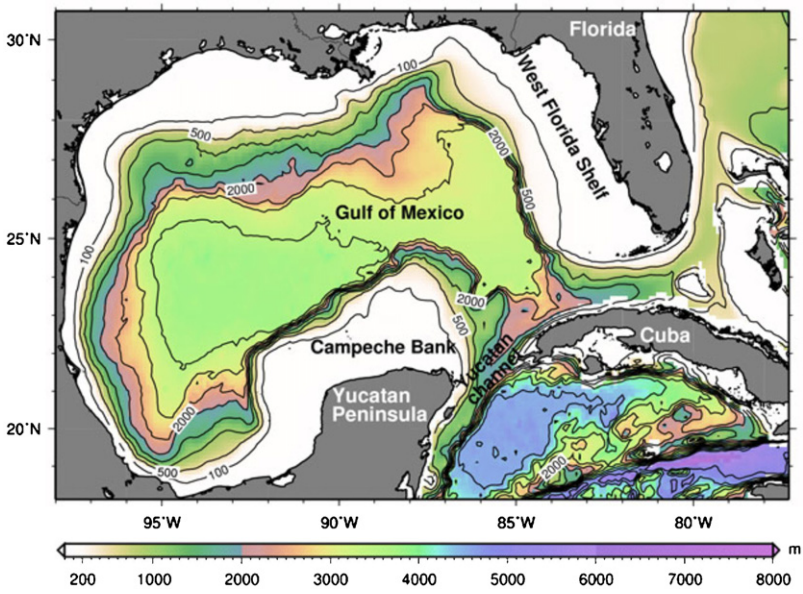

Fig. 2. The Gulf of Mexico modeling domain and topography (depth color scale in m).

the velocity field (Piterbarg et al., 2007). This corresponds to a predictability limit of about 1.5–6 days, smaller values for coastal regions near the Mississippi Delta and larger values for sub-surface deep water regions of the Gulf of Mexico. New data for the location of the oil spill must be fused with model predictions so that the model-estimated location of the oil spill does not diverge too far from reality. However, reliable identification of oil location is hampered by clouds that obscure satellite-based visible images, non-optimal wind regimes for SAR oil detection, and rough, rainy conditions for in situ observations. Another difficulty is whether no oil means that the area was reliably observed and no oil was found or that no observations were available in that region. Section 3 details our methodology for initializing an oil spill forecast model. The results of our simulations are shown and discussed in Section 4.

2. Model description

2.1. Hydrodynamic model

The HYbrid Coordinate Ocean Model, hereafter HYCOM, is a generalized hybrid coordinate ocean model developed by the HYCOM Consortium (http://hycom.org). The model vertical coordinate is isopycnal in the open stratified ocean; either z-level or terrain-following in shallow coastal regions, and z-level in the surface mixed layer. This generalized vertical coordinate approach is dynamic in space and time via the layered continuity equation, which allows a smooth dynamical transition between the coordinate types (Chassignet et al., 2003, 2006, 2007; Halliwell, 2004, 2009). The regional Gulf of Mexico HYCOM (GoM-HYCOM) is run in real time at the Naval Oceanographic Office (NAVOCEANO) DoD Supercomputing Resource Center (DSRC) by Pat Hogan and Ole-Martin Smedstad using atmospheric forcing from the Navy Operational Global Atmospheric Prediction System (NOGAPS). The model set-up is similar to Prasad and Hogan (2007). The horizontal resolution is 0.04° with 20 vertical layers. The model domain with bathymetry is shown in Fig. 2. The model has a realistic coastline with the minimum depth of 2 m. Boundary conditions are provided by a synoptically forced, lower resolution (0.08°) North Atlantic HYCOM model. Fields were averaged at the GoM-HYCOM boundaries to compute a model generated climatology in the Loop Current inflow through the Yucatan peninsula

and the Florida Current outflow through the Straits of Florida and adjacent passages between Cuba and the Bahamas (Kourafalou et al., 2009). Vertical mixing is provided by the K-Profile Parameterization (KPP) scheme (Large et al., 1994).

The data assimilation is performed using the Navy Coupled Ocean Data Assimilation (NCODA) system (Cummings, 2005) with a model nowcast used as the first guess. NCODA assimilates available satellite altimeter observations (along track obtained via the NAVOCEANO Altimeter Data Fusion Center), satellite and in situ sea surface temperature (SST) as well as available in situ vertical temperature and salinity profiles from XBTs and moored buoys. (ARGO floats are assimilated but are rarely present in this model domain.) Because there are significant time delays for observations to be made available on the GTS server for assimilation, a five-day old nowcast is used as the first guess for each forecast cycle, which is sufficient time for all altimetry observations to be made available. In order to examine the impact of data assimilation on the accuracy of model computed velocity fields (which were used for the trajectory modeling, see Section 2.2), a twin experiment with no data assimilation (free-running) was also performed. The free-running case uses the same initial and boundary conditions as the data assimilation simulation but no data are assimilated during the simulations.

2.2. Lagrangian trajectory modeling

The hydrodynamic model code allows the computation of particle trajectories using the HYCOM model Lagrangian particle package developed at the University of Miami. The particles are moved by both geostrophic and wind-driven ageostrophic currents plus an additional stochastic component represented by a Lagrangian stochastic model (LSM). The trajectory model advects particles using a fourth-order Runge–Kutta horizontal interpolation of the velocity field and was initially used for Lagrangian studies in a high-resolution MICOM simulation of the Atlantic Ocean (Garraffo et al., 2001). This trajectory model was implemented in HYCOM with multiple choices of vertical motion (advection by w, constant isopycnal surface, constant pressure surface) and the capability to sample model fields. This model was used to study the upper-limb pathways of the Atlantic Meridional Overturning Circulation by Halliwell et al. (2003). An offline version of this code with the LSM included was used for this study. Constant pressure floats were released in the top model layer in all of the two-dimensional oil spill trajectory forecast experiments reported here.

LSMs have been widely used in oceanography and meteorology to represent the unresolved velocity variability in ocean currents and winds, respectively. A random flight model is chosen to model both the unresolved ocean currents and wind speeds. In the *random flight* model (Griffa, 1996) the velocity field is expanded into deterministic $\bar{u}(x, t)$ and stochastic $u'(r, t)$ components, as $u = \bar{u} + u'$. The deterministic component $\bar{u}(x, t)$ is given by the GoM-HYCOM simulations. The stochastic component $u'(r, t)$ is modeled by a first-order auto-regressive (AR(1)) or Markovian process,

$$u'(r, t_k) = u'(r, t_{k-1}) \left(1 - \frac{\Delta t}{T_L}\right) + \sigma_u \sqrt{\frac{2\,\Delta t}{T_L}}\,\eta \tag{1}$$

where $\Delta t = (t_k - t_{k-1})$ is the time step, η is a unit-variance white noise process, σ_u is root mean square (rms) of the fluctuating velocity component u, assumed here to be 10 cm/s for the ocean component, and T_L is the Lagrangian integral time scale whose value is 3 days in the simulations presented below. A similar decomposition with the same paramter values is also performed for v. These LSM parameter values are based on estimates from Ohlmann and Niiler (2005).

In addition to this LSM, it was necessary for this study to develop a new component to the Lagrangian particle code to parameterize the nonconservative behavior of oil. A Monte Carlo method was introduced into the particle model code to represent weathering, mostly evaporation, sinking, biodegradation, and oil removal. Evaporation/sinking of this type of light crude is estimated to be about 30% of the oil in a week after surfacing. 5% of the oil sinks to the bottom and 5% dissolves over time (Scholz et al., 1999). Skimming and burning of the oil by workers is believed to have removed on the order of 10% of the oil (Lubchenco et al., 2010). All these oil removal processes are assumed to be unknown, completely random, and will be parameterized by a single number in our Monte Carlo resampling scheme. The rate of particle removal is controlled by a number c such that $0 < c < 1$. If c

is large, evaporation/oil removal is fast and if c is small, oil particles are around for a longer time. At each time step and for each particle, a uniform random number generator selects a random number RN between 0 and 1. If $RN < c$, then the particle is removed; otherwise, it is not removed. For example, if $c = 0.01$, 1% of the particles on the average would be removed at each time step. Let n equal the total number of time steps in a week, let s equal the percentage of particles that are removed in one week, then $c = O(s/100n)$. Based on the combined oil removal effects noted in the introduction, c needs to be selected so that at least 50% of the particles are removed after a week. Experiments with different values of c are shown and discussed in Section 4. The particle removal rate parameter c can be generalized to be temperature- or wind-dependent, as well as a function of the particle's age or oil state as for the three-dimensional simulations, but a constant c was adapted for the first set of two-dimensional oil trajectory simulations.

For the three-dimensional Lagrangian oil trajectory model where the oil particles can have three different states, three different particle removal rates were assumed corresponding to a 1/2-life of 10 h, 50 h, and 250 h for light, medium, and heavy oil, respectively. In addition, a biodegradation term was formulated to model the removal of oil by bacteria and it is a very slow function of the temperature and salinity with a time scale of years. The values of all of these parameters are chosen to within an order of magnitude and thus require further evaluation.

3. Initial conditions and oil source

The initialization of the Lagrangian trajectory model requires the position of all oil particles at the start of the model integration. These ICs were determined by blending the oil location information from all available observation-based analyses. The Deepwater Horizon surface oil spill had many characteristics that permitted identification from satellite including distinct color, surface reflectance, wave dampening characteristics, and sea surface temperature. The satellite, aerial, and in situ observations of the surface oil, especially when oil hit the coast, are abundant relative to subsurface observations. The U.S. National Oceanic and Atmospheric Administration (NOAA), the University of Miami's Center for Southeastern Tropical Advanced Remote Sensing (CSTARS), Roffer's Ocean Fishing Forecasting Service, Inc. (ROFFS^{TM}), the University of South Florida (USF), to name a few sources, all produced maps of surface oil locations. In general, infrared and ocean color satellite images, derived from polar orbiting NOAA satellites ($NOAA_{15}$, $NOAA_{16}$,$NOAA_{17}$, $NOAA_{18}$, and $NOAA_{19}$), NASA (Aqua and Terra) and European ($Metop_A$) satellites, were used to identify and track the water masses in the Gulf of Mexico. These satellite data along with data derived from satellite based synthetic aperture radar (TerraSARX, Envisat, Radarsat1, Palsar, Ers2, and $CosmoSkymed_1$,$CosmoSkymed_2$,$CosmoSkymed_3$), have a variety of spectral signals (infrared, near infra-red, visible, RGB, radar), as well as, a relatively high spatial resolutions of 75 m to 1 km, to visualize the surface oil and follow the water masses associated with the spill. Surface oil could be identified using a combination of SAR and visible-RGB with and without sun glint. The surface oil slick was very evident in clear satellite images in the visible part of observing spectrum, as well as in SAR images during times of optimal wind speed, and infra-red measurements, especially after particles surface. The different imagery provide complementary data and by studying the different images and image composites in a sequential manner one can follow the these water masses over hours, days, and weeks (Acker et al., 2009; Roffer et al., 2006).

The ICs for the two-dimensional model were calculated by specifying the locations of individual surface oil particles based on the observations. The ICs for the three-dimensional model also required specifying the state of the oil via its density, the size of the oil particles, and since it a three-dimensional Lagrangian trajectory calculation, the subsurface distribution. The primary contribution to the subsurface distribution is the gusher itself. Two release methods were used together to model the input of oil into the GoM for the two-dimensional Lagrangian trajectory model. The predominant "initial release" method was to release a large number of oil particles at an initial time with the density and distribution based on maps produced by fusing the different observations. Please see Figs. 1 and 3–6 for examples of these products and the resulting ICs. The second release method was to "continuously" release oil particles at the location of the Deepwater Horizon rig, latitude 28.74°N and longitude 88.39°W, as our model for an oil gusher source. Given the qualitative nature of the initial part of the investigation and the uncertainty in oil flow rates, eight oil particles were released in our two-dimensional simulations

every 3 h throughout the duration of the spill. The two-dimensional Lagrangian trajectory simulations are used to illustrate how the horizontal spread of the oil plume is sensitive to different particle removal rates provided by the Monte Carlo method and, as expected, to the ICs.

Given the day-to-day difficulty in observing the oil distribution, a fusing procedure that blends the visible oil distributions from various sources on a given day with the oil distribution on that day predicted by the prior model run, or alternately with the most recent good observations on days with bad observing weather should be used to construct the initial conditions. Only observations are used for the ICs of the particle locations in the simulations presented here. The basic premise for our method for fusing observations of oil location is that if any observation detects oil, it should be included since oil detection can be severely hampered by weather. The possibility of this fusing procedure over-estimating the size of the oil spill can be reduced if at least two observations (or model predictions in a more general setting) are required for reliable specification of oil at that location on that day. On the other hand, given that weather events reduce the chance of detecting oil and the finite in situ resources, this leads to an under-estimate of oil locations that can be partially compensated for by a data fusing technique. The initial conditions for our simulations were produced from superimposing digitizations of all estimates for a given day from CSTARS, ROFFS, and USF. NOAA estimates are used as a truth field to validate the simulations. If no data were available on a day, multi-day data composites were used. Given that the oil spill location data show regions with both thick oil and regions with oil/water/tar ball mixtures, the different regions, corresponding to high oil and low oil concentrations, were digitized separately. Visual inspection and comparison to other estimates, including the NOAA forecasts and the Lagrangian trajectory forecasts of our group and other groups at the University of South Florida and Florida State University, of the resulting oil locations maps were also consulted. A shape file was digitized from the oil analysis map and a polygon filling program generated longitude and latitude points inside the oil spill region. Particles at a large density of 10,000 per square degree were used for locations with high oil concentration and a particle density of 625 per square degree for locations with light oil (see Fig. 3 for an example). The two-dimensional Lagrangian simulations were initialized with these particle location maps, particles were added at the gusher site throughout all runs, every time step in short simulations and every 3 h in the longer time simulations, while particles were removed at each time step by the Monte Carlo scheme.

4. Lagrangian trajectory simulations

4.1. Two-dimensional simulation of oil particle trajectories

Figs. 4–8 are particle trajectory simulations performed by the UM/RSMAS Coastal and Shelf Modeling Group using the two-dimensional Lagrangian trajectory mode and output from the regional GoM-HYCOM. Other simulations and details are available at http://coastalmodeling.rsmas.miami.edu/Models/View/DEEPWATER_HORIZON_OIL_SPILL.

Fig. 4 shows different initial conditions and the distribution of particles from a "continuous" surface release of eight particles above the Macondo well location every 3 h from April 20th to May 14th with either no particle removal/evaporation, slow particle removal, or fast particle removal. The time for one-half of the particles to be removed is 120 h or 5 days for slow evaporation case, while the 1/2 life is 60 h or 2.5 days for the fast evaporation case. Even though the simulation lacks some of the oil that spread to west and toward the Mississippi Delta, that is seen in the oil location maps (Fig. 4), the estimated oil locations from the model are in good qualitative agreement with the data. The simulation of Lagrangian trajectories with no evaporation clearly over-estimates the amount of oil that is estimated on May 14, 2010 by either NOAA, ROFFS^{TM}, and CSTARS. The simulation with no particle evaporation has too many particles that are wrapped around the eastern flank of an eddy. The distribution of particles for the fast evaporation case agrees the best with both NOAA and CSTAR oil location estimates. This rate of particle removal/"evaporation" is commensurate with our estimates of oil removal rates by weathering and by in situ oil removal operations.

A series of ten-day Lagrangian simulations following the oil spill were performed; we will discuss an example for the time period July 12–22, 2010. We note that this is a tough test for model predictions, since ten days is greater than 4–6 days corresponding to twice the Lagrangian integral scale. Liu et al.

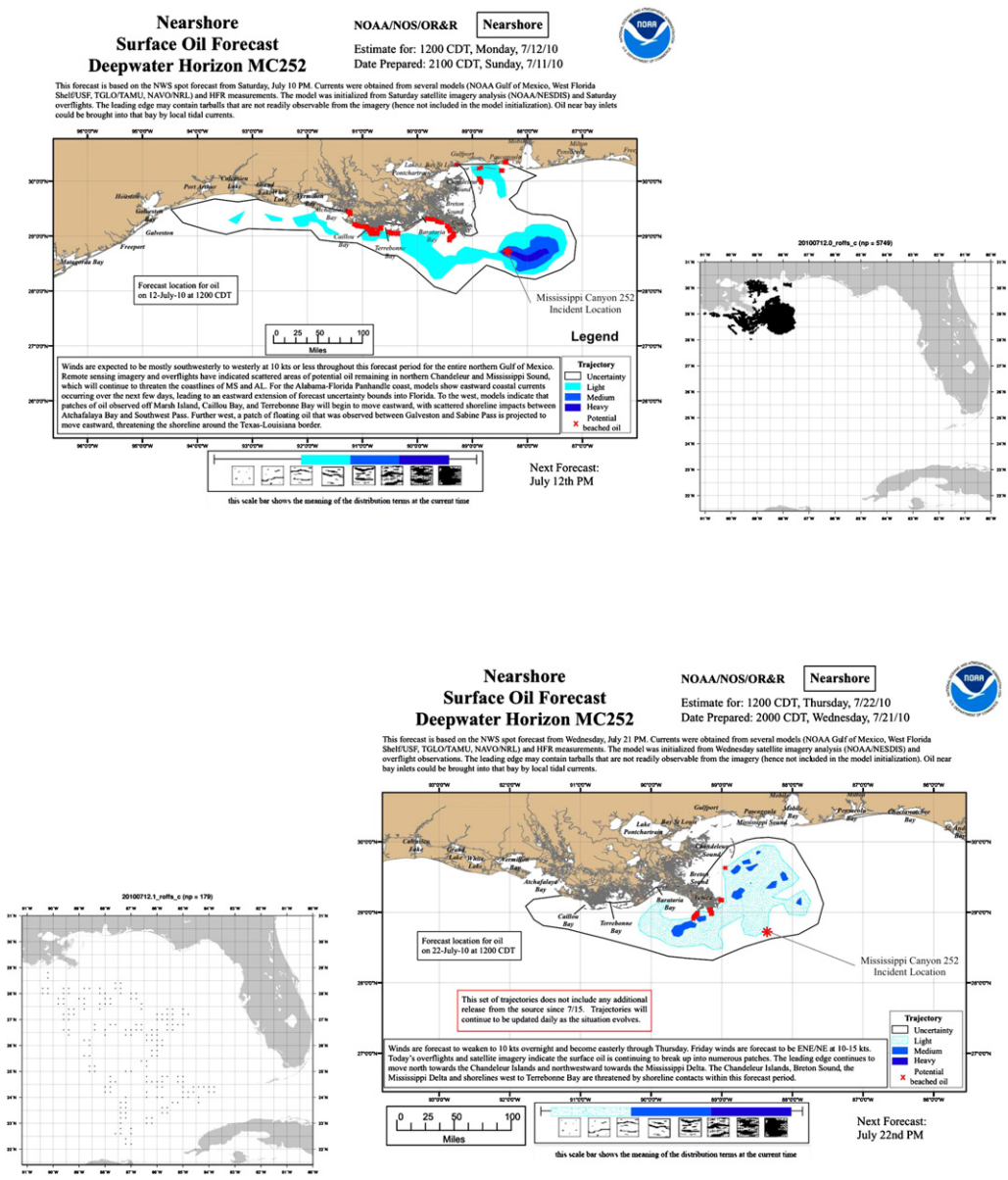

Fig. 3. The top left panel is NOAA's 24 h operational forecast of oil location for July 12, 2010, while the top right and bottom left panels are the near-field and far-field oil estimates from ROFFS^{TM} for the same day. The bottom right panel is NOAA's 24 h operational forecast of oil location for July 22, 2010.

(2011) also performed a qualitative analysis but with six different modeling systems and reached a similar conclusion that there was not much skill in predicting oil locations after a few days. Our goal is to elucidate some of the processes that impacted the transport and fate of oil particles. We have employed a series of simulations to examine the impact of data assimilation, model initialization and particle removal rate on the predicted trajectories. We have used either the free-running (Figs. 5 and 6) or data assimilative (Figs. 7 and 8) GoM-HYCOM simulations. We present the particle pathways during

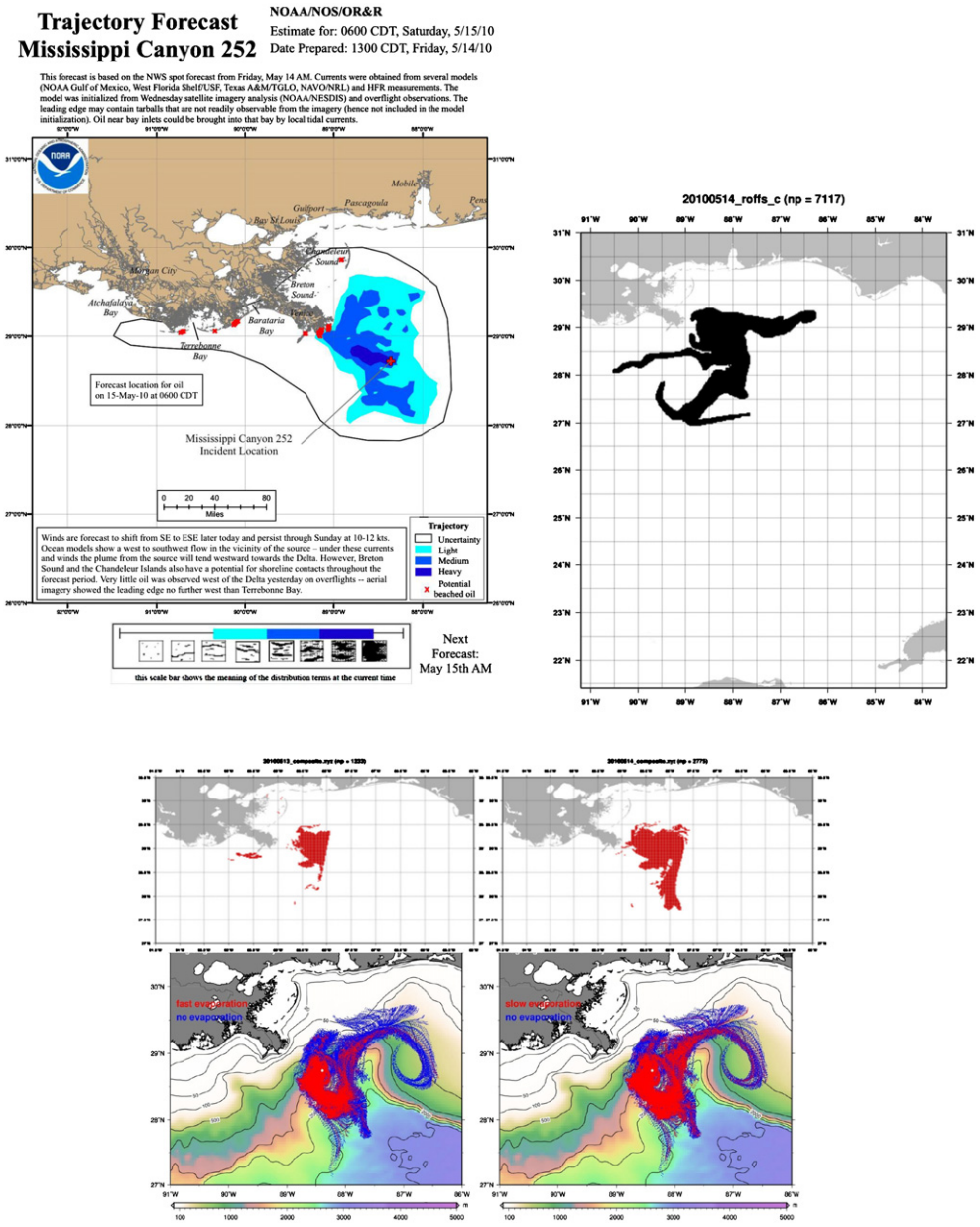

Fig. 4. The top left panel is NOAA's estimate of oil location for May 14, 2010, while the top right panel is an estimate from ROFFS™. The middle panels are oil location maps from CSTARS; and are based on a composite of SAR images for that day. The middle left panel is May 13, 2010 and there is an obvious swath discontinuity on the eastern edge of the blow. The middle right panel is the May 14, 2010 composite of SAR data and the westernmost oil from the day before is missing. Two model simulations, with a continuous particle release at the Macondo well location (marked with a white circle) are illustrated in the bottom panels. In both simulations, the no evaporation case is shown in blue and slow (lower left panel) and fast (lower right panel) evaporation in red. Depth contours and depth ranges are also plotted in the lower panels (depth color scale in m).

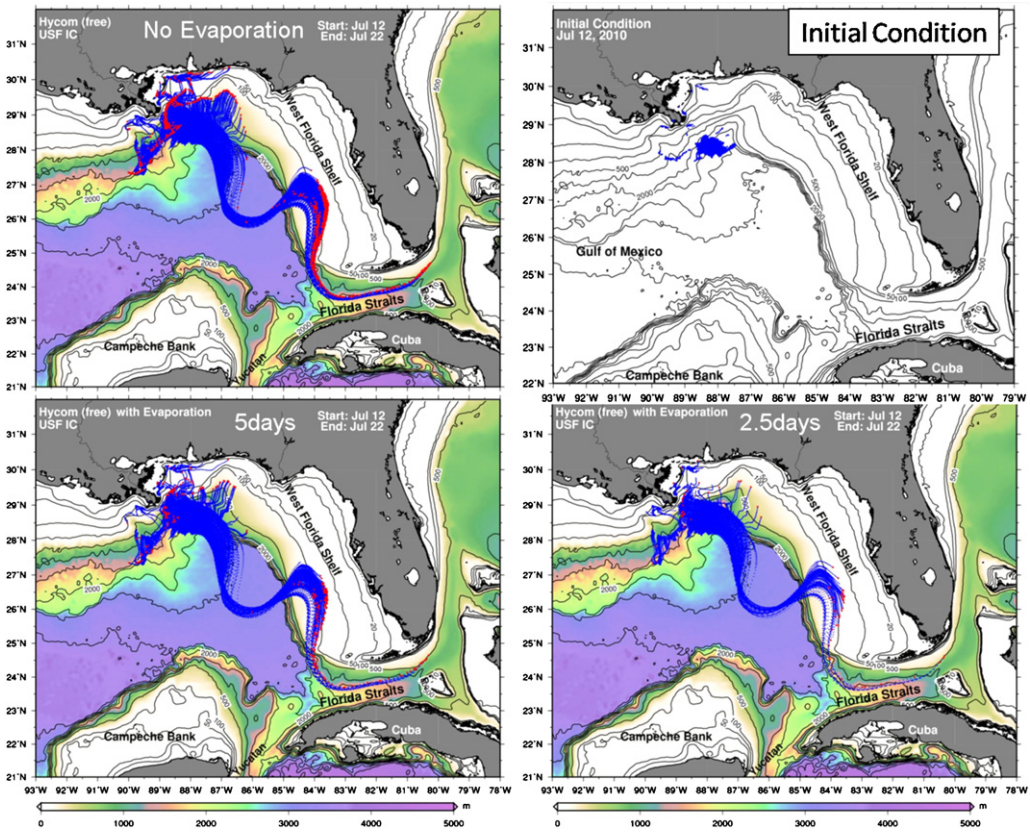

Fig. 5. Results using free-running hydrodynamic model velocities. The IC based on a satellite analysis provided by C. Hu (USF) for July 12, 2010 is plotted in the top right panel. The other 3 panels are maps of particle pathways during the 10-day simulations (blue) and their final position at the end of day 10 (red) for 3 different rates of evaporation. The upper left panel has no evaporation, the lower left panel is the slow evaporation rate (5.0 days) and the lower right panel is the fast evaporation rate (2.5 days) simulation.

the 10-day simulations and their final position at the end of day 10. Two different sets of ICs, provided by C. Hu (USF) (Figs. 5 and 7) or by ROFFS^{TM} (Figs. 6 and 8) are used in the simulations presented next. One day trajectory predictions from NOAA of the oil location for the starting and ending date of the simulations are given in Fig. 3. We note certain differences in the two sets of observational composites that we are using to initialize the Lagrangian predictions. There is more oil in both the near field and in the far field in the ROFFS^{TM} analysis, although the far field has very few particles. Observational limitations are an issue, especially in distinctions of pure oil and water and oil mixtures. Our goal is not to determine which of the ICs is better, but to illustrate the impact of differences in observational analyses on model forecasts.

The free-running GoM-HYCOM had the Loop Current well extended in the Gulf in the summer of 2010, which had a resemblance to the actual situation, but was over-extended, at close proximity to the Northern GoM shelf and the oil spill location. Regardless of evaporation rate and initial condition, a large number of particles was entrained into the Loop Current with some oil entering the Florida Current (Figs. 5 and 6). Without particle removal, a number of particles were quickly transported northward as part of the Gulf Stream current system. Fast evaporation rate (2.5 days) was more effective than slow evaporation rate (5 days) in limiting the amount of particles advected toward the Gulf interior and beyond. With the ROFFS ICs, more particles were specified to be already entrained in the Loop Current system, so the above pathways were amplified. These results had serious errors, as there

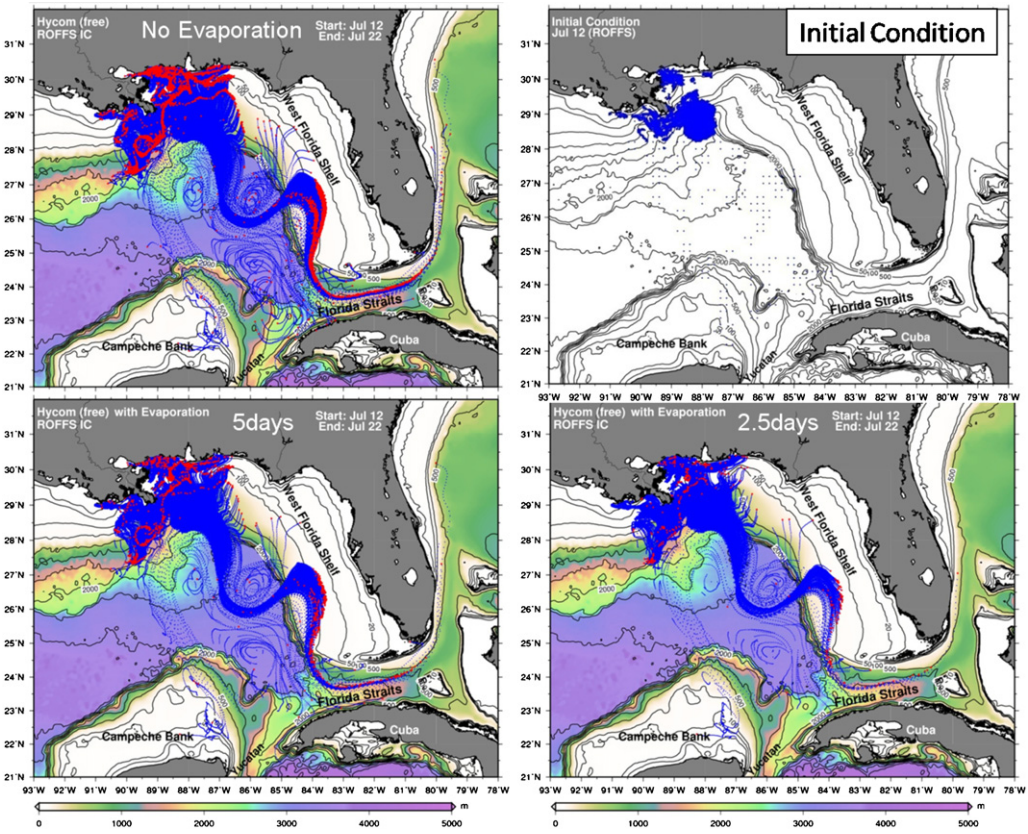

Fig. 6. Results using free-running hydrodynamic model velocities. The IC based on ROFFS^{TM} analysis for July 12, 2010 is plotted in the top right panel. The other 3 panels are maps of particle pathways during the 10-day simulations (blue) and their final position at the end of day 10 (red) for 3 different rates of evaporation. The upper left panel has no evaporation, the lower left panel is the slow evaporation rate (5.0 days) and the lower right panel is the fast evaporation rate (2.5 days) simulation.

were no official reports of oil offshore of Florida's east coast at this time (Fig. 3). In all cases a small number of particles crossed the western Gulf shelfbreak and showed tendency to travel across the West Florida Shelf. In the case of maximum number of particles remaining in the domain (ROFFS ICs and no evaporation, Fig. 5), traces along Northwestern Cuba, the Florida Keys and Florida Bay were also found.

The data assimilative GoM-HYCOM had the Loop Current in the right position, with a considerably smaller extension than in the free-run. Regardless of initialization, the vast amount of particles remained in the Northern Gulf area (Figs. 7 and 8), spreading toward along isobaths in a good representation of what was observed (Fig. 3). Particles already present in the Loop Current system (ICs from ROFFS) remained in the large scale current system and traveled toward the west Florida shelf and the Florida Straits. The increased amounts of oil present in ROFFS is probably due to their oil tracking algorithm relying too much on persistence advection of oil and no sinks of oil. This also led to an overestimation of oil impacting the shoreline when using ICs from ROFFS. However, there was a significant underestimation of oil near the coastline when using the USF oil spill location estimate for initialization. For both set of initial conditions, the fast evaporation rate and using velocity fields from a data assimilative model was found to produce the best results.

Our results illustrate some of the challenges for the prediction of oil pathways: observational issues, such as the accurate estimate of the oil patch; modeling issues, where velocities from data assimilative

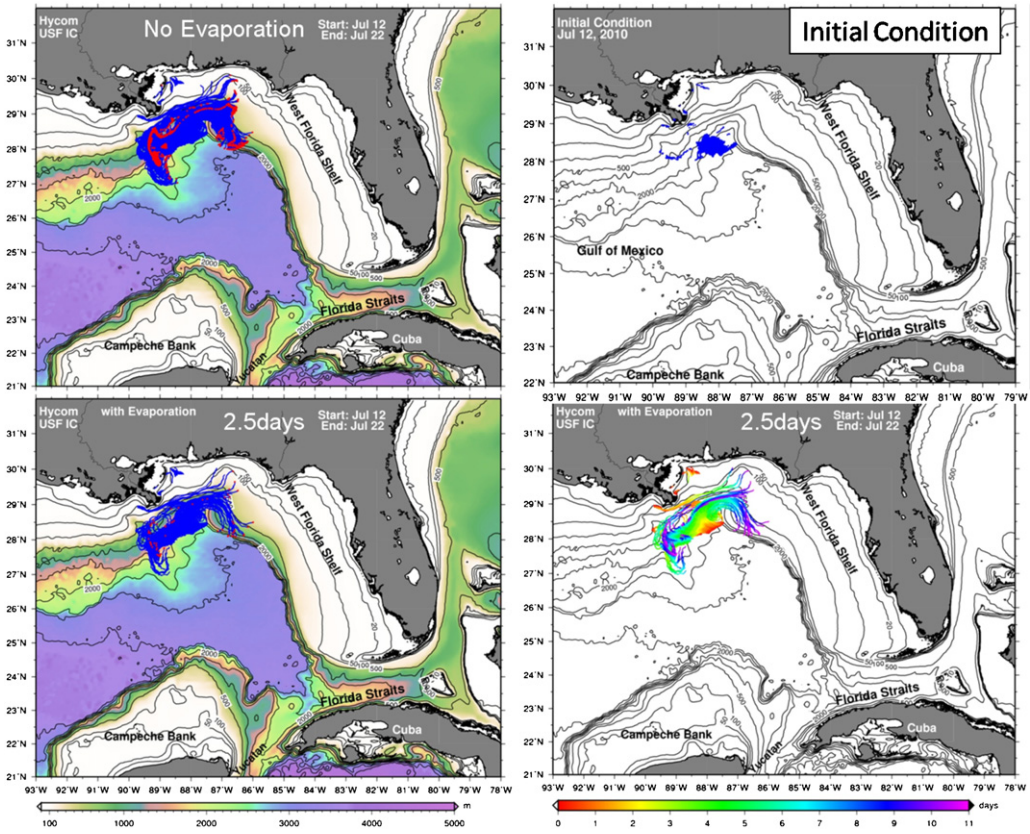

Fig. 7. Results using data assimilative hydrodynamic model velocities. The IC based on a satellite analysis provided by C. Hu (USF)^{TM} analysis for July 12, 2010 is plotted in the top right panel. The left panels are maps of particle pathways during the 10-day simulations (blue) and their final position at the end of day 10 (red) for 2 different rates of evaporation. The upper left panel has no evaporation, the lower left panel is the fast evaporation rate (2.5 days) simulation. The lower right panel is the number of days it takes (under fast evaporation conditions) for particles to reach their destination (color scale is days from 1 to 11).

hydrodynamic models offer a significant improvement of the background flow; technical issues that are hard to parameterize, such as oil booning and removal near the shoreline. The nonconservative behavior of oil makes the tracking and prediction more difficult than tracking of conservative water masses. It is well-known that particle trajectories are sensitive to ICs and the differences between Figs. 5 and 6 and between Figs. 7 and 8 highlight the difficulty in making operational predictions given large uncertainty in ICs. Oil particles approached the Loop Current system and some were entrained in our simulations. There was some observational evidence from ROFFS^{TM} analysis that oil substances were, indeed, entrained in the LCE, but there was no in situ validation of this. It should be noted that oil was detected in the far field at other times, *e.g.* on June 8, 2010 at 26°45.85′N, 86°03.65′ W (Wood, 2010). The differences between the slow and fast evaporation cases is the extent of dispersion with, of course, the faster evaporation case exhibiting less dispersion and less trajectories in the far field. Comparisons for other time periods yielded similar results.

4.2. Three-dimensional simulation of oil particle trajectories

Given the uncertainty in oil flow rates, evaporation rate, settling rate, winds, and ocean currents, a multi-dimensional set of parameters should be included in the Monte Carlo simulations for more accu-

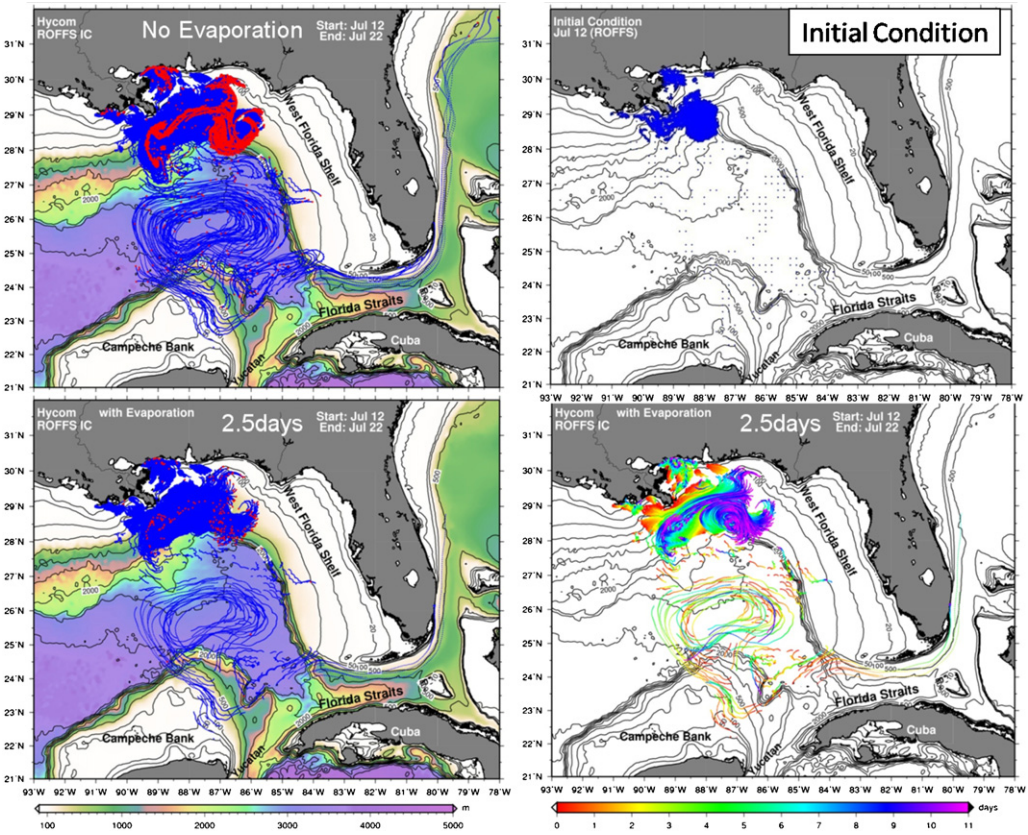

Fig. 8. Fig. 7 results using data assimilative hydrodynamic model velocities. The IC based on ROFFS^{TM} analysis for July 12, 2010 is plotted in the top right panel. The left panels are maps of particle pathways during the 10-day simulations (blue) and their final position at the end of day 10 (red) for 2 different rates of evaporation. The upper left panel has no evaporation, the lower left panel is the fast evaporation rate (2.5 days) simulation. The lower right panel is the number of days it takes (under fast evaporation conditions) for particles to reach their destination (color scale is days from 1 to 11).

rate estimates oil location via ensemble averaging. This simulation requires additional and expanded super computing resources, as compared to the hydrodynamic and particle model simulations presented in the previous sections. The primary differences are that the advanced Lagrangian model uses multi-state particles, three-dimensional currents, wind advection set to 1% of wind speed to incorporate a Stoke's Drift component from wave-induced motion, more realistic oil properties, and huge numbers of released particles proportional to the estimated flow rate. 10,000 particles were released every 30 min at a depth of 1200 m where the plume of mixed oil and gas is estimated to split into individual oil droplets and gas bubbles (*Pers Comm* Pete Cayragher, BP geologist). Each particle represents a fraction of the mass of the oil released and the number of particles released is adjusted so that each particle represents about 1 kg of oil. The oil properties such as the hydrocarbon fractions and the droplet size distribution at the source are two of the most crucial parameters affecting the time-varying footprint of oil in the water column. $O(10^7)$ particles were released in a 85 day model simulation. The model assumes that the oil is composed of three fractions, light, medium and heavy. The droplet (particle) sizes are assigned randomly between an assumed minimum and maximum values. In this study, as we are interested in examining the long-term budget of oil depending on its ability to stay at depth, only modeled oil droplets with diameter ranging from 1 to 300 μm are employed. This range allows studying particles that will remain at depth, as well as those that will raise rapidly to the surface. Particles larger than 300 μm are considered to reach the surface so quickly that their

size does not influence their fate. The model also includes the effects of evaporation and degradation due to physical and biological processes. These effects are parameterized based on the half-life times of the particle state. Only particles at the surface are subject to evaporative decay, while particles at all depths are subject to degradation. Srinivasan et al. (2010) details the computational aspects and error analysis of this large simulation.

Results of the three-dimensional Lagrangian model simulation are shown in Fig. 10. These simulation results are based on running 36 different simulations that differ with respect to the type of oil particles seeded as the oil source at depth. Both oil droplet size and the fraction of oil that corresponds to the 3 states (light, medium, and heavy oil) are varied from realization to realization. These two parameters were picked to be the perturbation source for the Monte Carlo simulations since this is the biggest unknown in this problem given the use of dispersants applied at the deep gusher and the lack of oil state data and they are important (Yapa and Chen, 2004). In contrast to the previous two-dimensional model simulations, this three-dimensional Lagrangian model simulation starts with particles at depth that rise to the surface driven by the imposed density differences and governed by turbulent mixing. Mixing is modeled using classical eddy diffusivity with $K_h = 10\,m^2/s^2$ and $K_z = 10^{-5}\,m^2/s^2$.

The light, medium, and heavy oil states correspond to densities of .78, .84, and .95 g/cm^3, respectively. The nominal density was set to .842 g/cm^3. A fraction of one oil was picked randomly to generate an initial ensemble and the other two were calculated by a weak constraint on the nominal density. No oil particle locations were specified at the surface in these trajectory simulations. The results for the fate of the oil for a three month simulation of the oil spill over its lifetime are shown in Fig. 9. The error bars are calculated based on polynomial chaos theory applied to the 36 Monte Carlo ensembles (Srinivasan et al., 2010). This calculation predicts that after 3 months, approximately 80% of the oil from the gusher below the depth of 800 m is gone and that 25% of the oil is still dispersed throughout the water column after 90 days, compared to the Lubchenco et al. (2010) estimate of 30%; surface evaporation removed 30% of the total oil, compared to 25% estimated by Lubchenco et al. (2010), and evaporation and other processes removed 99% of the surface oil so that only 1% of the oil is left on the surface. These calculations suggest that biodegradation throughout the water column was effective as surface evaporation at removing the oil. More realizations of this Monte Carlo simulation would lower the error bounds and change these estimates.

5. Discussion

The 2010 GoM oil spill was both a tragedy on many levels, as well as, an opportunity for ocean modelers to put their knowledge to the test on a highly visible and important practical problem. The first issue that was obvious is that the skill of any type of climatological winds and ocean currents for predicting Lagrangian motion is low. Climatological predictions had oil throughout the Gulf Stream system and into the North Atlantic (not shown), but this was not observed. The value of regional models (with improved resolution and topography) in regional forecasts was demonstrated here, by the official NOAA forecasts, and by other groups Liu et al. (2011). It was also demonstrated that the forecasts were better if the Eulerian velocity fields used to advect the Lagrangian particles were from data assimilative hydrodynamic models. Fig. 10 shows the root-mean-square (rms) position prediction error of the simulated trajectories at 15 m depth, and average distance travelled by both the model and in situ drifters, using AOML's drifters as both truth and to determine the launch location of the model simulated or synthetic drifters. These statistics were calculated over a three-month window beginning on June 13, 2010 with synthetic drifters "deployed" every 7 days at in situ drifter locations in the Gulf of Mexico east of 92°W, resulting in a total of 221 releases. Fig. 10a shows that data assimilation reduced the rms Lagrangian position error by 57% for 12 h prediction, by 50% for two day predictions, and with a 25% reduction in error and an average error of less than 20 km/day after 7 days. Fig. 10b shows that the velocity fields from data assimilative models over-smooths the Lagrangian trajectory, presumably because of Eulerian velocity fields that are smooth due to lack of high resolution data. Some preliminary calculations (not shown) have demonstrated that local, in situ data velocity data from either an array of floats or velocity profilers can further reduce the error by another 25%. Liu et al. (2011) also used

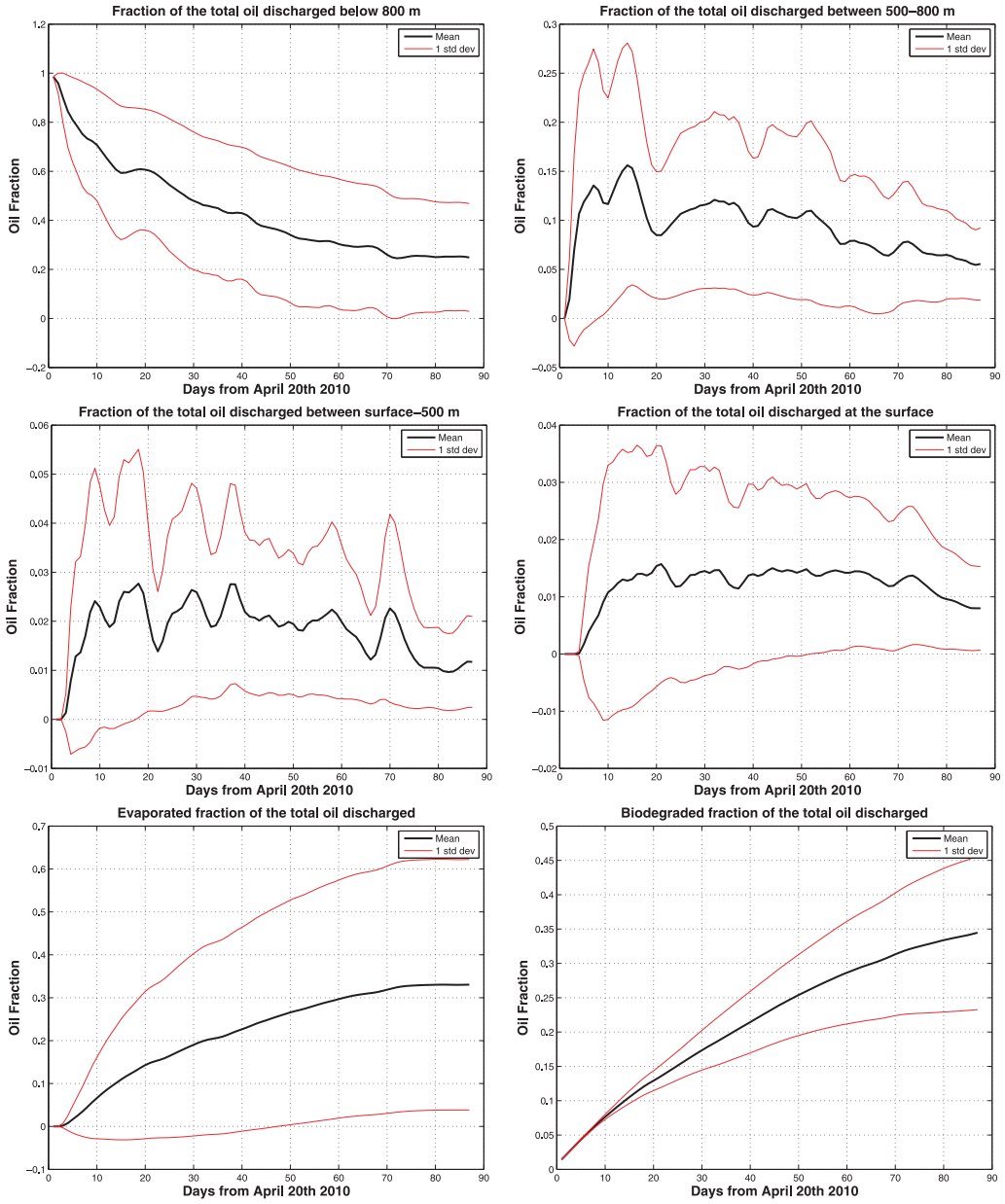

Fig. 9. Summary of the computed oil fate. The panels show the time history of the oil in the water column at different depths and the oil fraction lost due to evaporation and biodegradation. These mean and standard deviations are based on 36 realizations of the oil model run for range of droplet sizes and oil properties. In the mean, evaporation and degradation together remove about 70% of the oil released by 80 days.

satellite images to initialize six different regional and global numerical ocean circulation models. Their study also concluded that more observations are needed for data assimilation, that all aspects of weathering must be taken into account, and that the state of the oil should be modeled. This study presents a model that starts to address the last two issues.

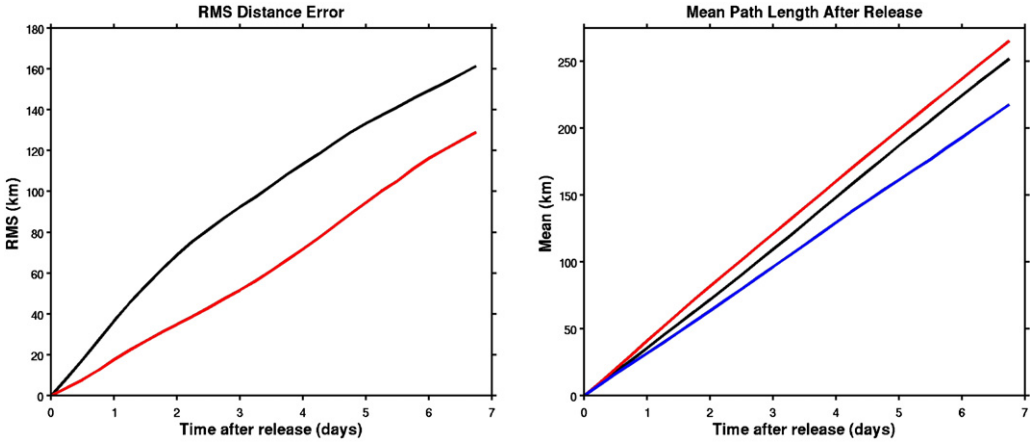

Fig. 10. (a) The left panel is the root-mean-square distance error between synthetic and real drifters for no data assimilation (black, top curve) and with data assimilation (red). (b) The right panel is the mean path length starting at release points for real drifters (black, middle curve), for synthetic drifters for no data assimilation (red, top curve) and with data assimilation (blue, bottom curve). (For interpretation of the references to color in this figure legend, the reader is referred to the web version of the article.)

In this paper, a method for producing ICs of oil location and a Monte Carlo method were introduced and evaluated to parameterize all oil removal processes such as evaporation. These simulations showed the well-known fact on the importance of ICs for good oil spill forecasts. The real-time determination of these ICs is hampered by many factors that are primarily economic/resource-rleated or related to atmospheric and oceanic variability. Liu et al. (2011) also stated besides the need for better ICs, there was also a need for better wind data for forcing circulation models. Real-time velocity data can make up for deficiencies in forcing, and optimal use of Lagrangian data (Chin et al., 2007; Molcard et al., 2007) can further reduce the model velocity and Lagrangian trajectory prediction error. Near the coast, HF radar would supply excellent data for assimilation. Given the similar performance of ocean circulation models (Liu et al., 2011) and that in a comparison of four advanced data assimilation schemes in the Gulf of Mexico (Srinivasan et al., 2011), all the methods produced similar results; it is the set of environmental data that is available that is the limiting factor for the success of a prediction scheme. This is well-known in operational weather forecasting, and in oceanography, introduced by Professor Allan R. Robinson over 30 years ago.

Two different oil spill trajectory modeling systems were presented with one system used for surface oil prediction given a set of ICs and another system that predicts the three dimensional oil distribution from a deep influx of oil particles of different sizes and densities. Both systems used Monte Carlo based methods because of the large amount of uncertainty in all components of the oil trajectory forecasting problem resulting from error in oil particle size composition, oil spill flow rate at source, operational wind and ocean current estimates, and in the observational oil location data that is amplified by the nonlinearity of the forward Lagrangian prediction problem. Though relatively elementary methods were used for combining the different observations and for oil weathering/removal, our maps produced the main features seen in the observations. The importance of using velocity fields from data-assimilative models for Lagrangian prediction was demonstrated. It should be noted that the paper focused on methodology, rather than aiming at accurate oil spill predictions, because of the inherent difficulty in the oil spill prediction problem. The uncertainties in input data that challenge such predictions were also discussed. Further improvements to the presented methodology would be a more general oil removal criterion, such as c being a function of oil age in the Monte Carlo oil removal algorithm, a Markov transition matrix between oil states, and improvements in how to fuse the model-based oil location estimates with observed locations. Recent studies by Spiller et al. (2008); Chin and Mariano (2010) shows that a nonlinear particle smoother would be a good choice for improv-

ing how model-based estimates and observed particle locations are fused. These and other modeling improvements will be the subject of future research.

Acknowledgements

We are grateful to Pat Hogan and Ole-Martin Smedstad (Naval Research Lab – Stennis Space Center) for providing the GoM-HYCOM velocity fields, to Chuanmin Hu (IMARS/USF) for providing one of the sets of satellite based oil particle locations used for the initial conditions, and to Rick Lumpkin for providing the drifter data for the model-data comparisons. The three-dimensional calculations were made possible by the University of Miami Center for Computational Science and we are very grateful for their support of our research. In recognizing the historical proportions of the Deepwater Horizon oil spill, the authors responded in real time as part of the oceanographic community's volunteer response. Partial support from the National Oceanic and Atmospheric Administration (NA10OAR4320143 to G. Halliwell, V. Kourafalou and A. Srinivasan) and the National Science Foundation (OCE0929651 to V. Kourafalou and OCE1048697 to C. Paris, V. Kourafalou and A. Srinivasan) are greatly appreciated. A. Srinivasan gratefully acknowledges the support of the U. of Miami Center for Computational Science.

References

Acker, J., Lyon, P., Hoge, F., Shen, S., Roffer, M., Gawlikowski, G., 2009. Interaction of Hurricane Katrina with optically complex water in the Gulf of Mexico: interpretation using satellite-derived inherent optical properties and chlorophyll concentration. IEEE Geosci. Remote Sens. Lett. 6 (2), 209–213.

Brekke, C., Solberg, A.H.S., 2005. Oil spill detection by satellite remote sensing. Remote Sens. Environ. 95, 1–13.

Camilli, R., Reddy, C.M., Yoerger, D.R., Van Mooy, B.A.S., Jakuba, M.V., Kinsey, J.C., McIntyre, C.P., Sylva, S.P., Maloney, J.V., 2010. Tracking hydrocarbon plume transport and biodegradation at Deepwater Horizon. Science 330 (6001), 201–204.

Chassignet, E.P., Smith, L.T., Halliwell, G.R., Bleck, R., 2003. North Atlantic simulations with the hybrid coordinate ocean model(HYCOM): impact of vertical coordinate choice, reference pressure and thermobaricity. J. Phys. Oceanogr. 33, 2504–22526.

Chassignet, E.P., Hurlburt, H.E., Smedstad, O.M., Halliwell, G.R., Hogan, P.J., Wallcraft, A.J., Bleck, R., 2007. Ocean prediction with the HYbrid Coordinate Ocean Model (HYCOM). J. Mar. Syst. 65, 60–83.

Chassignet, E.P., Hurlburt, H.E., Smedstad, O.M., Halliwell, G.R., Hogan, P.J., Wallcraft, A.J., Bleck, R., 2006. Ocean prediction with the Hybrid Coordinate Ocean Model (HYCOM). In: Chassignet, E.P., Verron, J. (Eds.), Ocean Weather Forecasting: An Integrated View of Oceanography. Springer, pp. 413–426.

Chin, T.M., Mariano, A.J., 2010. A particle filter for inverse Lagrangian prediction problems. J. Atmos. Oceanic Technol. 27, 371–384.

Chin, T.M., Ide, K., Jones, C.K.R.T., Kuznetsov, L., Mariano, A.J., 2007. Dynamic consistency and Lagrangian data in oceanography: mapping, assimilation, and optimization schemes. In: Griffa, A., Kirwan, D., Mariano, A.J., Ozgokmen, T., Rossby, T. (Eds.), Lagrangian Analysis and Predictability of Coastal and Ocean Dynamics. Cambridge University Press, pp. 204–230.

Cummings, J.A., 2005. Operational multivariate ocean data assimilation. Quart. J. Roy. Meteorol. Soc. 131D, 3583–3604.

Deepwater Horizon MC 252 Response Unified Area Command, 2010. Strategic Plan for Sub-Sea and Sub-Surface Oil and Dispersant Detection, Sampling, and Monitoring , November 13.

Garraffo, Z., Mariano, D.A.J., Griffa, A., Veneziani, C., Chassignet, E.P., 2001. Lagrangian data in a high resolution numerical simulation of the North Atlantic. I: Comparison with in-situ float data. J. Mar. Syst. 29, 157–176.

Griffa, A., 1996. Applications of stochastic particle models to oceanographic problems. In: Adler, R., Muller, P., Rozovskii, B. (Eds.), Stochastic Modelling in Physical Oceanography. Birkhauser Boston, Cambridge, MA, pp. 113–128.

Halliwell, G., 2004. Evaluation of vertical coordinates and vertical mixing algorithms in the hybrid-coordinate ocean model (HYCOM). Ocean Model. 7, 285–322.

Halliwell Jr., G.R., Weisberg, R.H., Mayer, D.A., 2003. A synthetic float analysis of upper-limb meridional overturning circulation pathways in the tropical/subtropical Atlantic. In: Malanotte-Rizzoli, Goni (Eds.), Interhemispheric Water Exchange in the Atlantic Ocean. Elsevier Oceanography Series, 68, pp. 93–136.

Halliwell, G.R., Barth, A., Weisberg, R.H., Hogan, P., Smedstad, O.M., Cummings, J., 2009. Impact of GODAE products on nested HYCOM simulations of the West Florida Shelf. Ocean Dyn., doi:10.1007/S10236-008-0173-2.

Hazen, T.C., Dubinsky, E.A., DeSantis, T.Z., Andersen, G.L., Piceno, Y.M., Singh, N., Jansson, J.K., Probst, A., Borglin, S.E., Fortney, J.L., et al., 2010. Deep-sea oil plume enriches indigenous oil-degrading bBacteria. Science 330 (6001), 204–220.

Kourafalou, V.H., Peng, G., Kang, H., Hogan, P.J., Smedstad, O.M., Weisberg, R.H., 2009. Evaluation of Global Ocean Data Assimilation Experiment products on South Florida nested simulations with the Hybrid Coordinate Ocean Model. Ocean Dyn., doi:10.1007/s10236-008-0160-7.

Labson, V.F., Clark, R.N., Swayze, G.A., Hoefen, T.M., Kokaly, R., Livo, K.E., Powers, M.H., Plumlee, G.S., Meeker, G.P., 2010. Estimated Minimum Discharge Rates of the Deepwater Horizon Spill – Interim Report to the Flow Rate Technical Group from the Mass Balance Team. USGS Open-File Report 2010-1132.

Large, W.G., McWilliams, J.C., Doney, S.C., 1994. Oceanic vertical mixing: a review and a model with a nonlocal boundary layer parameterization. Rev. Geophys. 32, 363–403.

Liu, Y., Weisberg, R.H., Hu, C., Zheng, L., 2011. Tracking the Deepwater Horizon oil spill: a modeling perspective. Eos Trans. AGU 92 (6), 45–46, doi:10.1029/2011EO060001.

Lubchenco J., McNutt, M., Lehr, B., Sogg, M., Miller, M., Hammond, S., Conner, W., 2010. Deepwater Horizon/BP Oil Budget: what happened to the oil? National Oceanic and Atmospheric Administration Report. Silver Spring, MD.

McNutt, M., Camilli, R., Guthrie, G., Hsieh, P., Labson, V., Lehr, B., Maclay, D., Ratzel, A., Sogge, M., 2011. Assessment of flow rate estimates for the Deepwater Horizon/Macondo Well Oil Spill. Flow Rate Technical Group report to the National Incident Command, Interagency Solutions Group, March 10, 2011.

Molcard, A., Ozgokmen, T.M., Griffa, A., Piterbarg, L.I., Chin, T.M., 2007. Lagrangian data assimilation in ocean general circulation models. In: Griffa, A., Kirwan, D., Mariano, A.J., Ozgokmen, T., Rossby, T. (Eds.), Lagrangian Analysis and Predictability of Coastal and Ocean Dynamics. Cambridge University Press, pp. 172–203.

NOAA, 2002. GNOME. General NOAA Oil Modeling Environment. User's Manual. Office of Ocean Resources Conservation and Assessment, National Oceanic and Atmospheric Administration, Seattle, Washington.

Ohlmann, J.C., Niiler, P., 2005. Circulation over the continental shelf in the northern Gulf of Mexico. Prog. Oceanogr. 64, 45–81.

Piterbarg, L.I., Ozgokmen, T.M., Griffa, A., Mariano, A.J., 2007. Predictability of Lagrangian motion in the ocean. In: Griffa, A., Kirwan, D., Mariano, A.J., Ozgokmen, T.M., Rossby, T. (Eds.), Lagrangian Analysis and Predictability of Coastal and Ocean Dynamics. Cambridge University Press, pp. 136–172.

Prasad, T.G., Hogan, P.J., 2007. Upper-ocean response to Hurricane Ivan in a 1/25° nested Gulf of Mexico HYCOM. J. Geophys. Res. 112, C04013, doi:10.129/2006JC003695.

Roffer, M.A., Gawlikowski, G., Muller-Karger, F., Schaudt, K., Upton, M., Wall, C., Westhaver, D.C., 2006. Use of thermal infrared remote sensing data for fisheries, environmental monitoring, oil and gas exploration, and ship routing. In: AGU Fall Meeting, San Francisco, CA, December.

Scholz, D.K., Kucklick, J.H., Pond, R., Walker, A.H., Bostrom, A., P. Fischbeck Scientific and Environmental Associates, 1999. Fate of Spilled Oil in Marine Waters. American Petroleum Institute Publication, 4691, p. 43.

Skognes, K., Johansen, O., 2004. Statmap-a 3-dimensional model for oil spill risk assessment. Environ. Model. Softw. 19 (7–8), 727–737.

Spiller, E.T., Budhiraja, A., Ide, K., Jones, C.K.R.T., 2008. Modified particle filter methods for assimilating Lagrangian data into a point-vortex model. Phys. D: Nonlinear Phenom. 237 (10–12), 1498–1506.

Srinivasan, A., Chassignet, E.P., Bertino, L., Brankardt, J.M., Brasseur, P., Chin, T.M., Counillon, F., Cummings, J., Mariano, A.J., Smedstad, O.M., Thacker, W.C., 2011. A comparison of sequential assimilation schemes for ocean prediction with the HYbrid Coordinate Ocean Model (HYCOM): twin experiments with static forecast error covariance. Ocean Model. 37 (3–4), 85–111.

Srinivasan, A., Helgers, J., Paris, C.B., LeHenaff, M., Kang, H., Kourafalou, V.H., Iskandarani, M., Thacker, W.C., Zysman, J.P., Tsinoremas, N.F., Knio, O.M., 2010. Many Task Computing for modeling the fate of oil discharged from the Deep Water Horizon well blowout. In: Many-Task Computing on Grids and Supercomputers (MTAGS), 2010 IEEE Workshop, 15 November, pp. 1–7.

Wood, M., 2010. Cruise Report: Deepwater Horizon Cruise – Rapid Gulf Survey: R/V Walton Smith Cruise – WS1010A. National Oceanic and Atmospheric Administration.

Yapa, Chen, 2004. Behavior of oil and gas from deepwater blowouts. J. Hydraul. Eng. 6 (540), 540–553, doi:10.1061/(ASCE)0733–9429(2004)130.